A Novel Image Compression Method Based on Coordinated Group Signal Transformation

Ekaterina Lopukhova , Grigory Voronkov * , Igor Kuznetsov , Vladislav Ivanov , Ruslan Kutluyarov , Elizaveta Grakhova

Posted Date: 30 April 2024

doi: 10.20944/preprints202404.1918.v1

Keywords: energy-efficient coding, differential coding, coordinated group signal transformation, image compression, image quality criteria, neural networks.

 doi:10.20944/preprints202404.1918.v1

Article

A Novel Image Compression Method Based on Coordinated Group Signal Transformation

Ekaterina Lopukhova [1], Grigory Voronkov [1,*], Igor Kuznetsov [1], Vladislav Ivanov [1], Ruslan Kutluyarov [1] and Elizaveta Grakhova [1]

School of Photonics Engineering and Research Advances (SPhERA), Ufa University of Science and Technology, 32 Z. Validi Street, Ufa 450076, Russia; lopukhova.ea@ugatu.su (E.L.); voronkov.gs@ugatu.su (G.V.); igor.kuznetsov-kiw@mail.ru (I.K); ivanov.vv@ugatu.su (V.I.); kutluyarov.rv@ugatu.su (R.K.); grakhova.ep@ugatu.su (E.G.)

* Correspondence: voronkov.gs@ugatu.su

Abstract: The paper describes the new method for image compression based on coordinated group signal transformation. The algorithm is a type of difference coding. Coordinated processing significantly simplifies the difference signal conversion scheme using a single group codec for all signals. The described method considers color channels as correlated signals of a multi-channel communication system. The specifics of the processed data required modification of the coordinated group processing algorithm. First, we changed how to calculate the difference signals to prevent data loss. Secondly, the group codec was supplemented with a neural network to improve the quality of reconstructed images. We considered the following types of neural networks: fully connected, recurrent, convolution, and convolution in the Fourier space. Based on the simulation results, it is best to use fully connected neural networks if the goal is to minimize processing delay time. These networks have a response time of 13 ms. On the other hand, if the priority is to improve quality in cases where delays are not critical, then convolution neural networks in the Fourier space should be used. These networks have a response time of 140 ms and are of significant interest.

Keywords: energy-efficient coding; differential coding; coordinated group signal transformation; image compression; image quality criteria; neural networks

1. Introduction

The amount of information generated worldwide has grown dramatically over the last few years. Wireless data traffic is a very illustrative example of this tendency. According to Ericsson data, global mobile data traffic (excluding traffic from fixed wireless networks) will grow to 288 EB per month by 2027. The total mobile monthly traffic, including fixed wireless networks, is forecast to grow to 370 EB by the end of 2027 [1]. Satellite traffic is projected to grow to 125 EB by 2030 [2]. At the same time, this data traffic extension was caused by the growth of wireless device numbers, not only user mobile terminals but also Internet of Things (IoT) equipment. The number of global active IoT connections grew by 18% in 2022 to 14.3 billion and is predicted to exceed 16.7 billion in 2023 [3]. For wireless networks (both terrestrial and satellite) and IoT devices the energy efficiency problem is critical, especially in 5G and 6G systems [4–7]. General approaches to reducing energy consumption and increasing energy efficiency in wireless networks are discussed in detail in [8], where, taking into account [9], it is indicated that improving algorithms and architecture devices and networks make the most significant contribution to energy savings (up to 75 %). In mobile networks, there are different algorithms to improve energy efficiency, such as MIMO, short-term sleep solutions, intra-sector traffic steering, and power control through random access channels [10,11]. Still, there are a lot of other approaches to solving the power consumption problem in wireless systems, such as applying multidimensional constellation diagrams [12,13] and minimum energy coding [14], and different types of precoding in high-throughput satellite communication systems [15].

 doi:10.20944/preprints202404.1918.v1

Coordinated group signal transformation (CGST), representing one of the energy-efficient coding methods, is another option to reduce the source signals average power. In contrast to existing difference coding methods based on predicting processed signals, including using neural networks [16,17], CGST is used for the collective processing of several correlated signals. This makes it possible to take into account their mutual connection and simplifies the coding scheme in a multi-channel system, that is, the codec structure. The performance of CGST has already been demonstrated for processing low-speed data [18], its effectiveness in increasing energy efficiency by reducing the amount of transmitted information (shortening the codeword length) was demonstrated in [19].

However, the prospects for using the CGST codec for high-speed multi-channel communication systems are of much greater interest. One of the possible applications is the satellite communication systems, which belong to an energy-deficient class. Thus, in this paper, we demonstrate the performance of the CGST codec in reducing the channel signals dynamic range when transmitting a color image of the earth's surface. To ensure maximum image quality at the codec output, we apply additional processing of the received images: the modified dynamic range reduction algorithm – to suppress unwanted brightness "zeroing" and postprocessing by the neural network – to decrease image blurring.

2. Group Signal Transformation Basics

The main idea of the CGST method is joint signal analysis in multi-channel systems to increase their performance. One way to achieve that is to combine the principles of differential pulse-code modulation (DPCM) with CGST, as is shown in Figure 1.

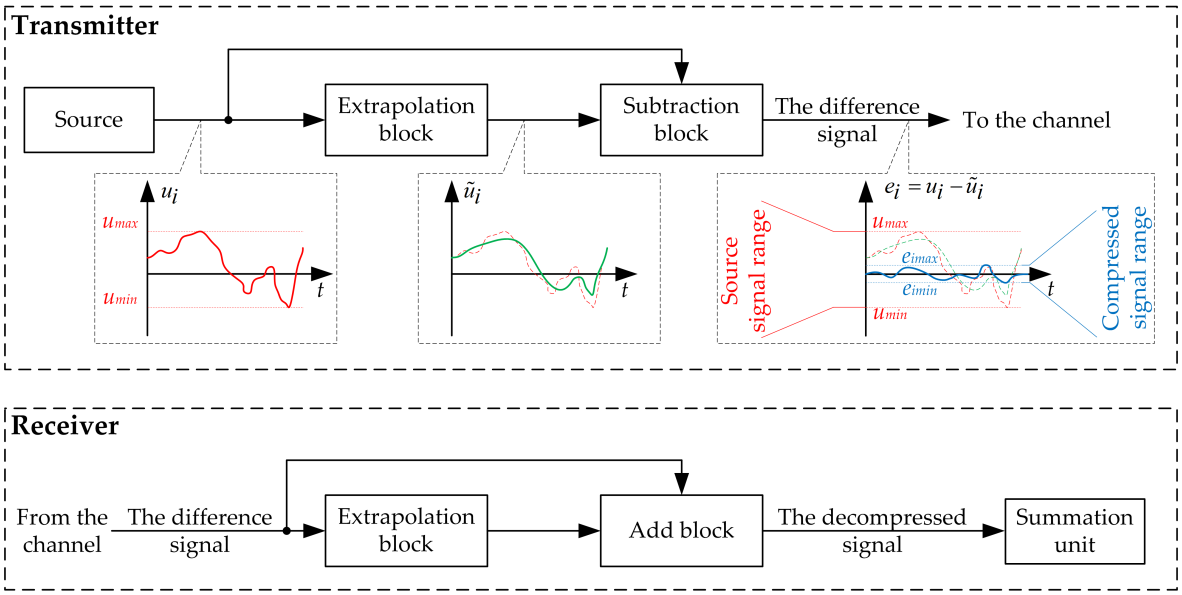

Figure 1. The concept of differential coordinated group transformation (illustration for a single channel of a multichannel system).

Following the approach, the original signals pass through the coordinated extrapolation block, the difference between the original signals and their estimates is calculated, and then the difference signals are used for processing and transmission. At the receiver, restoring the original signals is performed with known parameters of the extrapolation block. The main problem is to synthesize the transfer function of the coordinated extrapolation block. It may be solved as an optimization problem, for example, based on Wiener or Kalman filtering [18,20,21], but this approach is challenging to implement due to computational complexity. Another method was suggested in [22], presenting a group codec scheme for a multi-channel system with semi-type channels (Figure 2).

 doi:10.20944/preprints202404.1918.v1

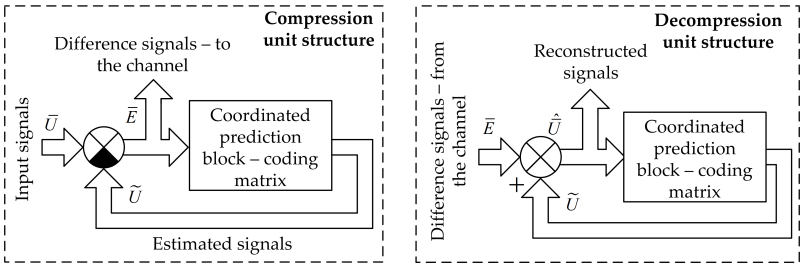

Figure 2. The structure of the transceiver channel using coordinated codec with a coding matrix.

The input vector $\overline{U} = [u_1, ..., u_n]$ (T is the transpose operator) excites the system. At the second input of the comparison elements, the signals $\widetilde{u}_i(t)$ (i - the channel number) passed through the coding matrix are applied. The vector of difference signals $\overline{E} = [e_1, ..., e_n]^T$, whose elements are determined by the expression $e_i(t) = u_i - -\widetilde{u}_i(t)$ is the output for the system.

Coordinating of neighboring channels is performed by the coordinated prediction block - coordinating matrix **K**, described as follows:

$$\mathbf{K} = \begin{bmatrix} k_{11} & k_{12} & \dots & k_{1n} \\ k_{21} & k_{22} & \dots & k_{2n} \\ \vdots & \vdots & \ddots & \vdots \\ k_{m1} & k_{m2} & \dots & k_{mn} \end{bmatrix}, \tag{1}$$

where k_{ii} elements are transmission coefficients in the direct branch located on the main diagonal, the elements k_{ij} (correlation coefficients) are determined by the following equation:

$$k_{ij} = \frac{1}{\sigma_i \sigma_j} \cdot \frac{1}{N} \sum_{t=1}^{N} (u_i - \overline{u}_i)(u_j - \overline{u}_j), \tag{2}$$

where σ – root-mean-square error of the channel signal, N – the number of signals' discrete when calculating the correlation in a discrete form.

The problem of coordinated system synthesis may be solved regarding the coefficients k of the main diagonal [22], allowing us to ensure the system's stability and, at the same time, to reduce the average signals' amplitude at the coder output. The roots of the characteristic equation are determined outside the circumference, which completely encompasses the system hodograph, which substantially simplifies the calculation: when defining the roots, the system's hodograph is replaced by a circle circumscribed about this hodograph.

3. CGST Codec Simulation for Processing Images

The hypothesis about the applicability of CGST for image compression is based on the fact that color channels can be considered as sources of correlated data since they describe a single object. In accordance with the number of color channels, the dimension of the CGST system also decreases; the correlation matrix, in this case, has a size of 3x3 and is determined as follows:

$$\mathbf{K} = \begin{bmatrix} k & k_{rg} & k_{rb} \\ k_{rg} & k & k_{bg} \\ k_{rb} & k_{bg} & k \end{bmatrix}. \tag{3}$$

The problem of effective image compression is one of the current research areas, for example, in satellite remote sensing systems [23]. Providing energy efficiency is also a great challenge for them. Therefore, we tested the effectiveness of the compression algorithm on images from the satellite remote sensing system. To do that, we obtained the data through the free navigation program SASGIS, which provides a way to download satellite images of the Earth's surface from many online mapping

 doi:10.20944/preprints202404.1918.v1

services. More specifically, we chose Yandex Maps, which acquires images from Ikonos, QuickBird, and WorldView2 satellites. An equilateral region was selected to form a dataset covering Ufa city (Russia, Republic of Bashkortostan) and an image matrix of 128x128 pixels. Based on those settings, we obtained 200 images.

As mentioned above, when using CGST for image compression, the input signals may be formed from its color channels, guaranteeing their correlation. So, the group codec processes the original images to reduce the signal's dynamic range. At the receiver, the images are restored using the inverse transformation. The value of the coefficient k in our simulation was chosen to reduce the dynamic range of signals by two times, that is, by 3 dB. Figure 3 shows the results of image compression for this case on each step.

According to the results, reducing the dynamic range of RGB channels by 3 dB or more using CGST inevitably introduces distortions in the transmitted information, mainly changing brightness. Due to the decrease in the brightness level of a certain number of pixels to zero during compression after the inverse transformation in the receiver, the resulting image is not identical to the original. In addition, extrapolation leads to undesirable image smoothing, which can be observed in Figure 3 at the output of the extrapolation block. In this regard, the image obtained at the codec output demonstrates a distorted color rendering due to the loss of brightness and blurring of the object's contours since the brightness values of the RGB channels are restored based on the channel signal passed through the extrapolation block.

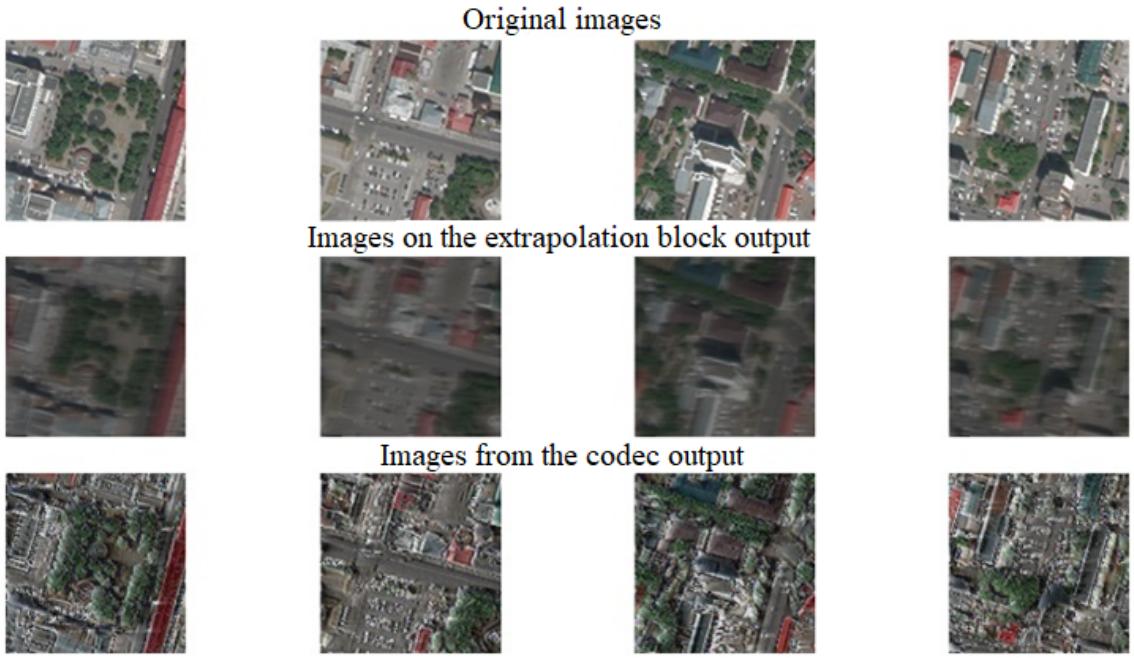

Figure 3. Images at some processing steps of the CGST codec.

3.1. CGST Algorithm Modification to Reduce the Distortions

As already mentioned, "zeroing" the brightness level of the picture's darker parts when compressing RGB channels in the correlation matrix by -3 dB or more made it impossible to restore the original information by the decoder with an appropriate quality. When completely dark areas appear in the compressed image in all three channels that are not present in the original image, it is essential to retain information about the level ratio of the original signal and the signal from the matrix output, which is achieved by fixing their positive difference value. Thus, we modified the original

 doi:10.20944/preprints202404.1918.v1

CGST algorithm. Before changes, the difference signal for the random channel at the coder output was determined by the following function:

$$e = \begin{cases} u - \widetilde{u}, u > \widetilde{u}, \\ 0, u < \widetilde{u}. \end{cases} \quad (4)$$

To avoid errors caused by "zeroing" according to equation (5), we modified the CSGT algorithm in the simulation as follows:

$$e = \begin{cases} u - \widetilde{u}, u > \widetilde{u}, \\ |u - \widetilde{u}| \cdot k_{red}, u < \widetilde{u}, \end{cases} \quad (5)$$

where k_{red} is the required coefficient of dynamic range compression, assumed to be 0.5 in the simulation. This modification to CGST ensures that the pixel brightness is not negative.

After passing through the extrapolation block and applying transformation (5), the areas near the object's edges in encoded images are significantly enhanced in brightness. At the same time, areas far from the borders remain with a lower brightness level. These signs indicate an increase in the image's spatial frequency. To test this assumption, we calculated the channel-averaged spatial frequency for the original image and one passed through the codec, which actually turned out to be higher for the latter. Chapter 3.2 provides a more detailed analysis of this issue.

3.2. CGST-Compressed Images Restoration Using Frequency Method

The problem of image blurring from the output of the extrapolation block can be leveled by applying image restoration methods after codec operation. However, the increased spatial frequency of processed images complicates analyzing the distorting function. It makes using classical approaches challenging due to the difficulties in determining the boundaries of objects and the simultaneous blurring of close-in-tone areas [24].

To ensure this, we applied a frequency method of image restoration known as a Gaussian low-pass filter to suppress edge effects. In a simulation, we used the standard deviation of the Gaussian distribution, which provides that the spatial frequency graphs of the original and processed images from the codec output almost coincide, as shown in Figure 4. As a result, the following processed images were obtained (Figure 5).

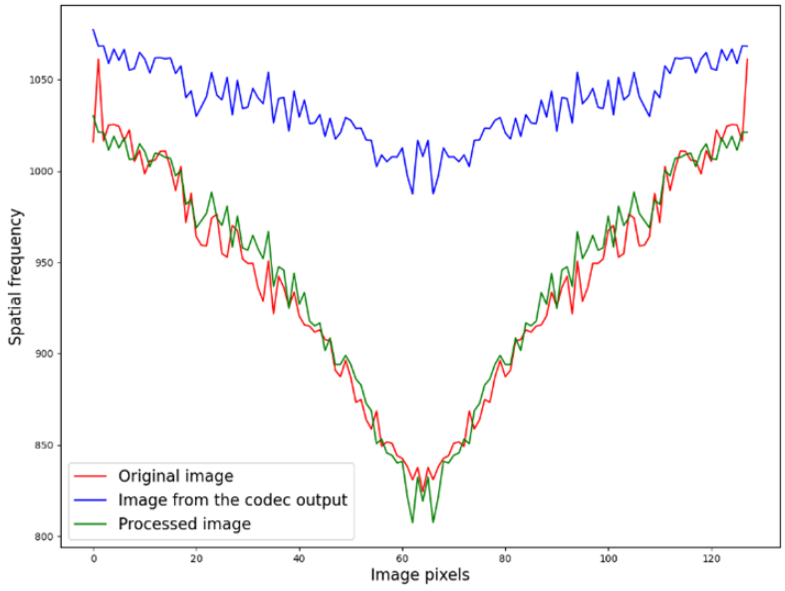

Figure 4. Spatial frequencies of the original (red), passed through codec (blue), and processed image (green).

 doi:10.20944/preprints202404.1918.v1

a b c

Figure 5. Image processing: (a) source image, (b) image after codec processing, (c) recovered image.

The recovered images' quality was tested according to the following criteria: the mean square error (MSE) and the Minkowski norm (MN) to check the proximity of the RGB channels' brightness levels; and structural similarity (SSIM) [25], which effectively reflects the structural distortions impact. However, the main disadvantage of the SSIM algorithm (in the spatial domain) is high sensitivity to scaling and image shift, which occurs when processing RGB channels with an extrapolation block. In this regard, another criterion was introduced – the SSIM extension to the region of the complex wavelet transform, i.e., complex wavelet SSIM (CW-SSIM), which is insensitive to non-structural distortions [26]. The averaged results of applying stated criteria for the restored images after the Gaussian filter within the entire dataset are presented in Table 1.

The results indicate only a slight improvement in image quality after filtering. While the effect of increased spatial frequency has been reduced, the decrease in the CW-SSIM indicates that the blurring present in the processed image has been worsened.

Thus, using the CGST codec for image processing leads to several distortions, conventional methods for eliminating which neutralize each other's effects. For example, applying a Wiener filter to an image Figure 5 after Gaussian low-pass filtering will reduce the blurring impact but increase the spatial frequency. As a part of this study, we decided to evaluate the possibility of restoring images after processing by neural network (NN) methods that are theoretically capable of adapting the mapping of input data to a given output space for any distortion model.

4. CGST-Compressed Images Postprocessing Using Neural Networks

One way to solve the distortions problem is to use a priori knowledge about the recovered image, for which supervised learning methods are applicable. With the accumulation of a sufficient amount of visual data, distorted information can be restored due to the generalizing ability of an intelligent algorithm. Such an approach showed excellent performance for restoring medical images, in which distortions expressed in local areas with noise and artifacts were caused by loss of information due to a decrease in the patient's radiation dose or an increase in the speed of tomography due to a reduction of the sampling rate [27–30].

Table 1. Image quality before and after filtering.

Metric	Source and receivedimages comparison without filtering	Source and received images comparison using filtering
MSE	43.9445	37.1378
MN	76.9161	67.5922
SSIM	0.0381	0.18605
CW-SSIM	0.5075	0.4779

One of the most popular and effective intelligent methods for improving image quality nowadays is the application of deep convolution neural networks (CNN) [31–34]. However, the response time of a NN, even if the structure is optimized, in most cases turns out to be too long for their implementation in real-time systems [35].

 doi:10.20944/preprints202404.1918.v1

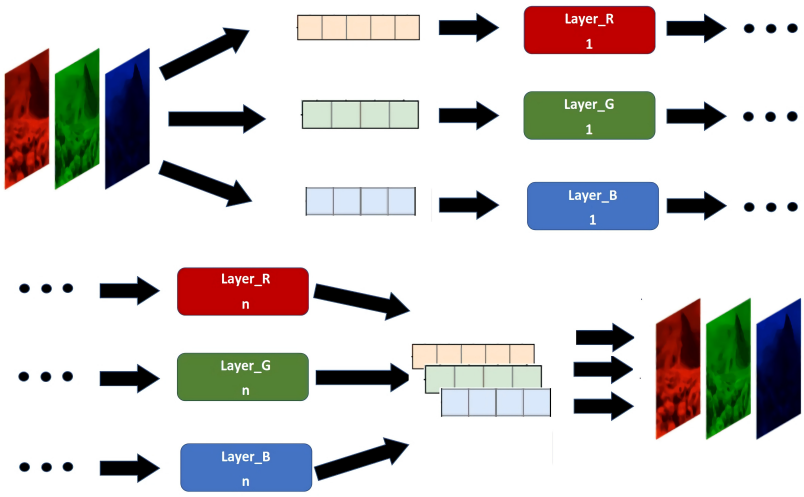

Figure 6. Neural network structure.

However, the NN operation time could be reduced when processing RGB channels instead of the image, simplifying the data to a vector of pixel brightness values. Based on video broadcast encoding delay requirements [36], the minimum decode delay is 133 ms at 30 fps or 160 ms at 25 fps. Also, with the Group-of-Pictures setting, these values are decreased to 33 ms and 40 ms respectively. Considering the average operating time of the extrapolation block and the encoding matrix on the receive, which equals 20 ms in simulation, the NN response time should be at most 113 ms at 30 fps and 140 ms at 25 fps (13 ms at 30 fps and 20 ms at 25 fps with the Group-of-Pictures setting).

The most commonly used NN types in image quality upgrade applications are fully connected, convolution, and recurrent. Another promising method is CNN, which parametrizes the hyperplane in the Fourier space and has shown less estimated time and greater accuracy than traditional CNN [37]. All of the above types of NN work effectively with a different number of free parameters and, therefore, with a various response time. Thus, the performance of different NN types strongly depends on settings and the number of frames per second.

The general logic of building the NN structure (Figure 6) was arranged in such a way as to process the vectors of RGB channel values in parallel, after which they were concatenated. By comparing the RGB channels for the image processed by the NN and the original image, we calculated the error function and then fixed the total error. The performance was estimated using the same image quality assessment metrics.

Considering the allowable image processing time, we used fully connected NNs with three hidden layers processing parallel the RGB channel, four-layer convolutional NN, and LSTM (long-term short-term memory) with three repeating layers. At the input and output of the NNs, we employed additional fully connected layers for concatenation and decatenation, respectively.

For NN training, the dataset was arranged from 200 images obtained via the SASGIS, 150 of which were assigned to the training set and 50 to the testing set. While training, the Adam optimization algorithm and the StepLR learning rate control function were used, which reduces the number of free parameters by a gamma with each epoch depending on the set image processing time (with or without the Group-of-Pictures setting). For all simulations, we used the set number of epochs in training equal to 100. The results of different algorithms are shown in Table 2.

To visually evaluate the performance of the applied NN structures, an example of the reconstructed image to varying values of SSIM is shown in Figure 7.

 doi:10.20944/preprints202404.1918.v1

a b c d

Figure 7. Applying neural networks results: a – source image; b – SSIM = 0.6553; c – SSIM = 0.7716; d – SSIM = 0.8082.

Table 2. Results of test image processing by trained NNs.

Neural network type	Response time, ms	MSE	MN	SSIM	CW-SSIM
Fully connected	13	36.214	67.014	0.1813	0.4493
	20	35.943	65.891	0.1875	0.4636
	113	31.212	58.337	0.2162	0.4845
	140	25.613	46.611	0.3688	0.5175
Recurrent	13	36.454	68.845	0.1802	0.4263
	20	29.814	42.674	0.4091	0.5343
	113	27.034	47.013	0.3825	0.5772
	140	22.613	37.421	0.6012	0.6553
Convolution	13	–	–	–	–
	20	30.614	57.437	0.2605	0.4858
	113	21.360	38.594	0.5790	0.6342
	140	18.714	34.803	0.6475	0.7716
Convolution in Fourier space	13	–	–	–	–
	20	–	–	–	–
	113	20.018	37.020	0.6047	0.6642
	140	17.810	33.331	0.6759	0.8082

The results in Table 1 and 2 allow us to draw the following conclusions. Using a neural network made it possible to simultaneously solve the issue of blurring images and changing spatial frequency. The most important, in our opinion, is the significant improvement in the CW-SSIM indicator since it is responsible for the visual correspondence of the reconstructed image to the transmitted one. The use of a fully connected neural network did not bring any improvements. However, recurrent and convolutional neural networks helped increase CW-SSIM by 0.15 and 0.27, respectively, at the maximum response time (140 ms), significantly improving the MSE and MN criteria. The convolutional neural network in Fourier space demonstrated the best results with CW-SSIM increase by 0.3. However, its advantage over the traditional convolutional neural network is insignificant (the improvement in the CW-SSIM metric was 0.03 with close MSE and MN values). At the same time, even the least efficient neural network (recurrent one) with a relatively simple architecture and NN response time as low as 20 ms provided more effective image quality restoration than traditional filtering.

5. Discussion

This paper presents a new image compression method based on the CGST algorithm. Its use for this purpose required some modifications. Firstly, it was proposed that the method of generating the difference signal be changed to exclude data loss ("zeroing" the brightness of pixels). Secondly, to combat the distortions introduced by CGST and improve the quality of the reconstructed images, the output signal of the CGST decoder was supplemented with a neural network since an analysis of these distortions showed that traditional methods for improving image quality are problematic. For example, a similar approach is used when restoring the quality of medical images. We formed a dataset of 200 remote sensing images available in open sources (the authors can provide the dataset upon request). This dataset size is sufficient for proof of concept since the number of specific image

 doi:10.20944/preprints202404.1918.v1

details determines the sample size. In the considered case (due to the effect introduced by distortions), such details are simple geometric figures that display the shapes of buildings, roads, and natural objects. When training the NN for the case of more specific details, it may be necessary to increase the size of the dataset, similar to the datasets for the analysis of medical images, with the complex nature of the extracted parameters.

The results obtained from the test data showed the possibility and expediency of using neural network methods to restore images in a satellite image transmission system that uses the method of coordinated group signal processing to improve energy efficiency. The joint use of CGST and neural network methods has demonstrated the possibility of reducing the dynamic range of the original signals by 3 dB, which decreases the number of transmitted bits by 1 for each code block while ensuring sufficient data recovery quality.

The time delays of 13 ms and 20 ms, in addition to the encoding time in video broadcasting, satisfy the requirements of acceptable delays in computer vision and virtual reality applications, as they are within the limits of the average processing time of visual information in the human brain [38]. It should also be noted that, due to the use of supervised learning methods, the applicability of the image restoration algorithm after codec operation is limited by the type of training visual information.

Besides working in low-speed information transmission systems, the algorithm of power-efficient coding with CNN can post-process images with higher accuracy in computer vision systems, medical diagnostics, and remote sensing of the Earth. At the same time, the limitation of the applicability of the above machine learning methods is the adaptation only to a certain distortion model, taken into account when training algorithms. One of the possible solutions to this problem is the combination of neural network methods with a more detailed analysis of the original images and distortion models during the training process.

Author Contributions: Conceptualization, G.V. and E.L.; methodology, I.K.; software, E.L.; validation, G.V., E.G. and R.K.; formal analysis, G.V. and R.K.; investigation, G.V, V.I. and E.L.; resources, R.K.; data curation, E.L.; writing—original draft preparation, G.V. and E.L.; writing—review and editing, E.G.; visualization, G.V.; supervision, E.G.; project administration, G.V.; funding acquisition, E.G. All authors have read and agreed to the published version of the manuscript.

Funding: This work was funded under the grant of the Russian Science Foundation (Project #21-79-10407).

Institutional Review Board Statement: Not applicable.

Informed Consent Statement: Not applicable

Data Availability Statement: A dataset for training the ML algorithm is available on request to the corresponding author's e-mail.

References

1. Ericsson Mobility Report November 2021. Available online: https://www.ericsson.com/4ad7e9/assets/local/reports-papers/mobility-report/documents/2021/ericsson-mobility-report-november-2021.pdf (accessed on 2024-03-26).
2. Halpin, S. Space Traffic Data Volumes Increase 14x Over the Next Ten Years. Available online: https://www.nsr.com/space-traffic-data-volumes-increase-14x-over-the-next-ten-years/ (accessed on 2024-03-26).
3. State of IoT 2023: Number of connected IoT devices growing 16% to 16.7 billion globally. Available online: https://iot-analytics.com/number-connected-iot-devices/ (accessed on 2023-12-13).
4. Alliance, B.N.; Hattachi, R.E.; Erfanian, J. *NGMN 5G White Paper*; NGMN, 2015.
5. Tong, P.Z.W., Ed. *6G: The Next Horizon: From Connected People and Things to Connected Intelligence*; Cambridge University Press, 2021. https://doi.org/10.1017/9781108989817.
6. Plastras, S.; Tsoumatidis, D.; Skoutas, D.N.; Rouskas, A.; Kormentzas, G.; Skianis, C. Non-Terrestrial Networks for Energy-Efficient Connectivity of Remote IoT Devices in the 6G Era: A Survey. *Sensors* **2024**, *24*, 1227.
7. Ledesma, O.; Lamo, P.; Fraire, J.A. Trends in LPWAN Technologies for LEO Satellite Constellations in the NewSpace Context. *Electronics* **2024**, *13*, 579.

 doi:10.20944/preprints202404.1918.v1

8. Alagoz, F.; Gur, G. Energy efficiency and satellite networking: A holistic overview. *Proceedings of the IEEE* **2011**, *99*, 1954–1979.
9. Nekoogar, F.; Nekoogar, F. *From ASICs to SOCs: a practical approach*; Prentice Hall Professional, 2003.
10. Sabella, D.; Rapone, D.; Fodrini, M.; Cavdar, C.; Olsson, M.; Frenger, P.; Tombaz, S. Energy management in mobile networks towards 5G. *Studies in Systems, Decision and Control* **2016**, *50*, 397–427. https://doi.org/10.1007/978-3-319-27568-0_17.
11. Holma, H.; Toskala, A. *LTE for UMTS : OFDMA and SC-FDMA based radio access*; Wiley, 2009; p. 433.
12. Markiewicz, T.G. An Energy Efficient QAM Modulation with Multidimensional Signal Constellation. *International Journal of Electronics and Telecommunications* **2016**, *62*, 159–165. https://doi.org/10.1515/ELETEL-2016-0022.
13. Li, W.; Ghogho, M.; Zhang, J.; McLernon, D.; Lei, J.; Zaidi, S.A.R. Design of an energy-efficient multidimensional secure constellation for 5G communications. *2019 IEEE International Conference on Communications Workshops, ICC Workshops 2019 - Proceedings* **2019**. https://doi.org/10.1109/ICCW.2019.8756862.
14. Peng, Y.; Andrieux, G.; Diouris, J.F. Minimization of Energy Consumption for OOK Transmitter Through Minimum Energy Coding. *Wireless Personal Communications* **2022**, *122*, 2219–2233. https://doi.org/10.1007/S11277-021-08989-W.
15. Khammassi, M.; Kammoun, A.; Alouini, M.S. Precoding for high throughput satellite communication systems: A survey. *IEEE Communications Surveys & Tutorials* **2023**.
16. Sheferaw, G.K.; Mwangi, W.; Kimwele, M.; Mamuye, A. Waveform based speech coding using nonlinear predictive techniques: a systematic review. *International Journal of Speech Technology* **2023**, pp. 1–29.
17. Anees, M. Speech coding techniques and challenges: a comprehensive literature survey. *Multimedia Tools and Applications* **2023**, pp. 1–21.
18. Voronkov, G.S.; Smirnova, E.A.; Kuznetsov, I.V. The method for synthesis of the coordinated group DPCM codec for unmanned aerial vehicles communication systems. *Proceedings - ICOECS 2019: 2019 International Conference on Electrotechnical Complexes and Systems* **2019**. https://doi.org/10.1109/ICOECS46375.2019.8950024.
19. Ivanov, V.V.; Lopukhova, E.A.; Voronkov, G.S.; Kuznetsov, I.V.; Grakhova, E.P. Efficiency Evaluation of Group Signals Transformation for Wireless Communication in V2X Systems. In Proceedings of the 2022 Ural-Siberian Conference on Biomedical Engineering, Radioelectronics and Information Technology (USBEREIT), 2022, pp. 167–170. https://doi.org/10.1109/USBEREIT56278.2022.9923401.
20. Voronkov, G.S.; Filatov, P.E.; Sultanov, A.K.; Voronkova, A.V.; Vinogradova, I.L.; Kuznetsov, I.V. Signals and messages differential transformation research for increasing multichannel systems efficiency. *Journal of Physics: Conference Series* **2018**, *1096*. https://doi.org/10.1088/1742-6596/1096/1/012175.
21. Voronkov, G.S.; Voronkova, A.V.; Kutluyarov, R.V.; Kuznetsov, I.V. Decreasing the dynamic range of OFDM signals based on extrapolation for information security increasing. *Proceedings - 2018 Ural Symposium on Biomedical Engineering, Radioelectronics and Information Technology, USBEREIT 2018* **2018**, pp. 271–274. https://doi.org/10.1109/USBEREIT.2018.8384602.
22. Voronkov, G.S.; Filatov, P.E.; Sultanov, A.K.; Kutluyarov, R.V.; Vinogradova, I.L.; Kuznetsov, I.V. Improving the efficiency of multichannel systems based on the coordination of channel signals. *Journal of Physics: Conference Series* **2019**, *1368*. https://doi.org/10.1088/1742-6596/1368/4/042047.
23. Zhang, B.; Wu, Y.; Zhao, B.; Chanussot, J.; Hong, D.; Yao, J.; Gao, L. Progress and Challenges in Intelligent Remote Sensing Satellite Systems. *IEEE Journal of Selected Topics in Applied Earth Observations and Remote Sensing* **2022**, *15*, 1814–1822. https://doi.org/10.1109/JSTARS.2022.3148139.
24. Gonzalez, R.C. *Digital image processing*; Pearson education india, 2009.
25. Wang, Z.; Bovik, A.C.; Sheikh, H.R.; Simoncelli, E.P. Image quality assessment: From error visibility to structural similarity. *IEEE Transactions on Image Processing* **2004**, *13*, 600–612. https://doi.org/10.1109/TIP.2003.819861.
26. Wang, Z.; Simoncelli, E.P. Translation insensitive image similarity in complex wavelet domain. In Proceedings of the Proceedings.(ICASSP'05). IEEE International Conference on Acoustics, Speech, and Signal Processing, 2005. IEEE, 2005, Vol. 2, pp. ii–573.
27. Pelt, D.M.; Batenburg, K.J. Fast tomographic reconstruction from limited data using artificial neural networks. *IEEE Transactions on Image Processing* **2013**, *22*, 5238–5251.

 doi:10.20944/preprints202404.1918.v1

28. Chen, H.; Zhang, Y.; Zhang, W.; Liao, P.; Li, K.; Zhou, J.; Wang, G. Low-dose CT via convolutional neural network. *Biomedical Optics Express*, *8*, 679. https://doi.org/10.1364/BOE.8.000679.
29. Wang, S.; Su, Z.; Ying, L.; Peng, X.; Zhu, S.; Liang, F.; Feng, D.; Liang, D. Accelerating magnetic resonance imaging via deep learning. In Proceedings of the 2016 IEEE 13th international symposium on biomedical imaging (ISBI). IEEE, 2016, pp. 514–517.
30. Schlemper, J.; Caballero, J.; Hajnal, J.V.; Price, A.; Rueckert, D. A deep cascade of convolutional neural networks for MR image reconstruction. In Proceedings of the Information Processing in Medical Imaging: 25th International Conference, IPMI 2017, Boone, NC, USA, June 25-30, 2017, Proceedings 25. Springer, 2017, pp. 647–658.
31. Gatys, L.A.; Ecker, A.S.; Bethge, M. Image Style Transfer Using Convolutional Neural Networks, 2016.
32. Dong, C.; Loy, C.C.; He, K.; Tang, X. Image Super-Resolution Using Deep Convolutional Networks. *IEEE Transactions on Pattern Analysis and Machine Intelligence* **2016**, *38*, 295–307, [1501.00092]. https://doi.org/10.1109/TPAMI.2015.2439281.
33. Ignatov, A.; Kobyshev, N.; Timofte, R.; Vanhoey, K.; Gool, L.V. DSLR-Quality Photos on Mobile Devices with Deep Convolutional Networks. *Proceedings of the IEEE International Conference on Computer Vision* **2017**, *2017-October*, 3297–3305. https://doi.org/10.1109/ICCV.2017.355.
34. Savvin, S.; Sirota, A. An Algorithm for Multi-Fame Image Super-Resolution under Applicative Noise Based on a Convolutional Neural Network. *Proceedings - 2020 2nd International Conference on Control Systems, Mathematical Modeling, Automation and Energy Efficiency, SUMMA 2020* **2020**, pp. 422–424. https://doi.org/10.1109/SUMMA50634.2020.9280698.
35. Vu, T.; Van Nguyen, C.; Pham, T.X.; Luu, T.M.; Yoo, C.D. Fast and efficient image quality enhancement via desubpixel convolutional neural networks. In Proceedings of the Proceedings of the European Conference on Computer Vision (ECCV) Workshops, 2018, pp. 0–0.
36. *Technical Report ITU-R BT.2044-0 (2004) Tolerable round-trip time delay for sound-programme and television broadcast programme inserts - Context and rationale*.
37. Li, Z.; Kovachki, N.; Azizzadenesheli, K.; Liu, B.; Bhattacharya, K.; Stuart, A.; Anandkumar, A. Fourier Neural Operator for Parametric Partial Differential Equations. *arxiv* **2020**, [2010.08895].
38. Potter, M.C.; Wyble, B.; Hagmann, C.E.; McCourt, E.S. Detecting meaning in RSVP at 13 ms per picture. *Attention, Perception, and Psychophysics* **2014**, *76*, 270–279. https://doi.org/10.3758/S13414-013-0605-Z/FIGURES/4.